# Seasonal and Interannual Variations of Yellowfin Tuna Catches along the Omani Shelf

# Saud Al Jufaili and Sergey A. Piontkovski\*

Sultan Qaboos University, P.O.Box 34, Muscat 123, Sultanate of Oman E-mails: sjufaily88@gmail.com; spiontkovski@gmail.com

#### **Abstract**

Yellowfin tuna contributed markedly to Omani catches of the past 30 years. However, artisanal catches vary over seasons and years, and induce economic losses. With this regard, the analysis of seasonal and interannual fluctuations of Yellowfin tuna catches was carried out, based on monthly and annual time series of 20 environmental variables. Data were subjected to the Principle Component Analysis and the Multiple Ridge Regression Analysis. It was shown that catches along the Omani shelf, in 1988-2018, were subjected to a human-induced and environmental forcing subjected to seasonal and interannual variations. Seasonal variations demonstrated a bimodal trend, with a major peak in April and a minor one in October, observed during spring and fall inter-monsoon seasons. Apart from the seasonality of fishing efforts associated with rough weather during the Southwest Monsoon, seasonal variations of catches were statistically related to 9 environmental variables (namely, the wind speed, zonal gradient of sea surface temperature, geostrophic current velocity, dissolved oxygen concentration and sardine catches (an indicator of food for tuna), the amount of mesoscale eddies, mixed layer depth, photosynthetically available radiation, and outgoing longwave radiation), that explained 71% of observed seasonal variations of the tuna catch. Due to the four-fold increase in fishing efforts, artisanal catches of Yellowfin tuna along the Omani shelf exhibited a two-fold increase over the past three decades. However, the catch per unit of effort did not show statistically confirmed increase for this time range. Interannual variations of catches exhibited an irregular pattern, with several peaks (in 1995, 2004 and 2018, with the later one still not resembled entirely). Statistical analysis implied 8 environmental variables, which modulated these variations: the wind

\_

<sup>\*</sup>Corresponding author

speed, amount of cyclonic eddies, sardines (an indicator of food resource for tuna), concentration of nitrates, atmospheric pressure gradient, sea surface temperature, El Niño-Southern Oscillation, and Indian Ocean Dipole anomalies. Coupling of these variables explained 70% of interannual variations of Yellowfin tuna catch along the Omani shelf overlooking the western Arabian Sea. The relationship between catches, El-Niño Southern Oscillation and Indian Ocean Dipole index pointed to a certain "numeric match" of two atmospheric anomalies that should happen, to favor maximal tuna catches.

#### INTRODUCTION

Yellowfin tuna (*Thunnus albacares* Bonnaterre 1788) comprises 42% of the total tuna catch of the Indian Ocean (http://asiapacfish.org/index.php/species/item/18-yellowfintuna). An artisanal fishery of Yellowfin tuna is substantial, accounting for catches over 200, 000 mt per annum during the past decade, where the proportion of this species in total catches increased from about 30% to nearly 50% (IOTC 2017). After Somalia and the Bay of Bengal, the Arabian Sea region is the third, based on its contribution to the total annual catch in the Indian Ocean. The sea is unique, in a sense of ocean-atmosphere interactions modulating the circulation affected by monsoonal winds. The monsoon-driven variability is pronounced in almost all key physical, chemical and biological characteristics featuring coastal and oceanic marine ecosystems (Banse and English, 2000; Barber et al., 2001).

In comparison to seasonal, the interannual variations were much less investigated, which is associated with a relatively short period of observations. As for the fishery, historical records of fish catches in Oman are among the most documented in the region. They are available from the 1980s up to the present time and were published by the Ministry of Agriculture and Fisheries, in the form of reports on monthly and annual landings (Fisheries Statistics Books). These reports characterize fishery along the 3,165 km coastline, with a commercial fishing area of 350,000 km<sup>2</sup>, in which the artisanal fishery accounts for 99% of total landings, with 49,715 fishermen employed in the fisheries sector operating 24,014 fishing boats 97 % of which are fiberglass boats 8-10 meters in length (Fisheries Statistics Book, 2018).

The total artisanal production of Omani large pelagic fishery in 2018 was 100,820 tons, with a total value of 1,008,202 Omani rials. Tuna products dominate the fish consumption in Oman (Mahrooqi and Al-Shidhami, 2013). The Yellowfin tuna contributed markedly to the Omani catches of the past 30 years. Interestingly, all "tuna regions" of the Indian Ocean have exhibited more or less similar fluctuations of catches over time, with an increase from 1950s to the peak in 1993-1995 and then low values to the second peak in 2004-2005, after which catches demonstrated a twofold decline (Herrera et al., 2012) and a subsequent gradual increase up to the present time. Marked seasonal and interannual fluctuations of large pelagic fish catches result in economic losses which could exceed one order of magnitude. For instance, the value of Yellowfin tuna catches in the southern part of Sharkiyah, in 2018 (one of the most

successful years of fishery), varied from 238 (RO 1000) in June to 2,257 (RO 1000), in April. Over years, the value varied from 836 (RO 1000) in 2010, to 13,144 (RO 1000) in 2018 (Fisheries Statistics Book, 2018).

An approximate match of interannual peaks of catches over regions in the western Indian Ocean points to a certain mechanism underlying this match on a basin scale. With this regard, we aimed to analyze seasonal and interannual fluctuations of Yellowfin tuna artisanal catches with special reference to a regional circulation and global scale atmospheric anomalies. In terms of the terminology involved, we followed Khalfallah et al (2016) who defined Omani catches as the sum of "landings" consisting of retained, landed and discarded catch.

#### **DATA AND METHODS**

General approach to data analysis was based on assembling monthly and annual time series of environmental variables potentially important for elucidation of factors affecting fish catches. These time series were subjected to the Principle Component Analysis and the Multiple Ridge Regression Analysis. A potential importance of variables selected for statistical analyses come from studies that highlighted the role of certain factors affecting spatial distribution and abundance of large and small pelagic fishes in the Indian Ocean (Lee et al., 1999; Mohri and Nishida, 2000; Stretta, 1991; Suzuki et al., 1978).

A set of variables selected for our study was contributed by the photosynthetically available solar radiation, outgoing longwave radiation, sea level pressure gradient, sea surface temperature gradient (off shore), zonal component of the wind speed, meridional component of the wind speed, Indian Ocean Dipole index, El-Niňo Southern Oscillation index, zonal component of the surface current velocity, meridional component of the surface current velocity, amount of cyclonic mesoscale eddies, amount of anti-cyclonic mesoscale eddies in the upper layer of the ocean, euphotic depth, mixed layer depth, concentration of dissolved oxygen, concentration of dissolved nitrates, concentration of chlorophyll-a (an indicator of phytoplankton biomass at the surface), sardine catches (an indicator of food source for tuna), and Yellowfin tuna catches.

Monthly and annual time series of the wind speed and outgoing longwave radiation were retrieved from the NCEP-NCAR reanalysis database (Table 1), which is a joint product from the National Center for Environmental Prediction (NCEP, USA) and the National Center for Atmospheric Research (NCAR, USA). The product represents gridded data on atmospheric and physical parameters worldwide, from 1948 to the present (Kistler et al., 2001). The wind speed field was characterized by the meridional and zonal components retrieved for the western Arabian Sea region limited by the 16°N and 22°N parallels and by 54-60°E meridians.

Time series on climate indices characterizing the Indian Ocean Dipole and the El-Niňo Southern Oscillation (El-Niňo 3.4 region -5°N-5°S, 120°-170°W) were assembled from appropriate databases (Table 1).

**Table 1.** Environmental variables used for the Principal Component Analysis, Multiple Stepwise Ridge Regression Analysis and plots.

Variable	Acronym	Time range	Data source
Gradient of atmospheric sea level pressure, mb	SlpG	1948-2018	http://www.esrl.noaa.gov/psd/data
Photosyntheticaly available radiation, Einstein m <sup>-2</sup> day <sup>-1</sup>	PAR	1997-2015	https://giovanni.gsfc.nasa.gov
Meridional component of the wind speed, m s <sup>-1</sup>	Mw	1948-2018	http://www.esrl.noaa.gov/psd/data
Zonal component of the wind speed, m s <sup>-1</sup>	Zw	1948-2018	http://www.esrl.noaa.gov/psd/data
Sea surface temperature gradient, °C km <sup>-1</sup>	GSST	1948-2018	http://www.esrl.noaa.gov/psd/data
Sea surface temperature, °C	SST	1948-2018	https://giovanni.gsfc.nasa.gov
Euphotic depth, m	EuD	1997-2015	https://giovanni.gsfc.nasa.gov
Mixed layer depth, m	MLD	1997-2015	https://giovanni.gsfc.nasa.gov
Meridional component of geostrophic current velocity, m s <sup>-1</sup>	McV	1992-2018	https://www.esr.org/research/oscar
Zonal component of geostrophic current velocity, m s <sup>-1</sup>	ZcV	1992-2018	https://www.esr.org/research/oscar
Amount of cyclonic eddies	CEd	1993-2018	https://www.aviso.altimetry.fr
Amount of anticyclonic eddies	AEd	1993-2018	https://www.aviso.altimetry.fr
Concentration of dissolved oxygen, ml L <sup>-1</sup>	Oxy	1960-2008	Regional database (Piontkovski and Al Oufi, 2014)
Concentration of dissolved nitrate, µmol L-1	NO3	1997-2015	https://giovanni.gsfc.nasa.gov
Concentration of chlorophyll-a, mg m <sup>-3</sup>	Chl	1998-2018	https://giovanni.gsfc.nasa.gov
Outgoing longwave radiation	OLR	1948-2018	http://www.esrl.noaa.gov/psd/data
El-Nino Southern Oscillation index	ENSO	1950-2018	https://www.esrl.noaa.gov/psd/data/cli mateindices/list/ https://origin.cpc.ncep.noaa.gov/produ cts/analysis_monitoring/ensostuff/ON I_v5.php
Indian Ocean Dipole index	IOD	1970-2018	https://www.esrl.noaa.gov/psd/gcos_w gsp/Timeseries/DMI/ http://www.jamstec.go.jp
Sardine landings, mt	Sard	1988-2018	Statistics Book, 2002-2018
Yellowfin tuna landings, mt	Tuna	1988-2018	Statistics Book, 2002-2018
Fishing effort	Fe	1988-2018	Statistics Book, 2002-2018

Data on zonal and meridional components of geostrophic sea surface currents were downloaded from the Ocean Surface Current Analysis Real-time database which contains near-surface ocean current velocity estimated from sea surface height,

surface vector wind and sea surface temperature. These data amalgamate various satellites and *in situ* instruments. Data are arranged in the form of a 1/3 degree grid with a 5 day resolution (https://www.esr.org/research/oscar/).

Maps of sea surface height anomalies were acquired from the CCAR Global Near Real-Time SSH Anomaly/Ocean Color Data Viewer and the AVISO server. Daily images retrieved with 4-km spatial resolution from MODIS-Aqua were used, to estimate the daily amounts of cyclonic and anticyclonic eddies in the region from 2002 to 2018. In following elements of the approach proposed by Chelton et al. (2011) and Arur et al. (2014), the outermost closed contour resembling a vortex with a minimum 5 cm amplitude, was identified as an eddy. Cyclonic eddies (with anticlockwise rotation) were characterized by negative sea surface height anomalies depressed in cores of eddies, while anti-cyclonic eddies (with clockwise rotation) have positive sea surface height anomalies elevated in cores, within the bounding contour.

Remotely sensed MODIS-Aqua products were employed, to retrieve monthly time series of the concentration of chlorophyll-*a*, dissolved nitrate, mixed layer depth, euphotic layer depth and sea surface temperature available from the NASA/Giovanni database as part of the NASA's Goddard Earth Sciences Data and Information Services Center. Data on sea surface temperature we used to estimate the sea surface temperature gradient (offshore, between two adjacent regions separated by a distance of one centigrade, on the map (Figure 1).

Data on seasonal variation of the dissolved oxygen concentration were retrieved from various expeditions carried out along the Omani shelf and highlighted elsewhere (Baird et al., 2009; Piontkovski and Al-Oufi, 2014). In particular, we analyzed vertical profiles of the dissolved oxygen concentration from five voyages of R/V "Mustagila1", which were carried out along the shelf in the 20-250m depth range, from the Ras al Hadd cape to the southernmost part of the Omani shelf (to the Yemen boarder), in 2007-2008. Conductivity, temperature, density, depth, and dissolved oxygen concentration were measured using an RBR CTD probe deployed from the vessel. ARGO floats data, from 2002 to 2015, were used to construct the T-S diagrams featuring the thermo-haline structure of water masses and currents, with a special reference the Oman Coastal Current to (http://www.argo.ucsd.edu/Argo data and.html).

Tuna are active migrants capable of covering thousand mile distances at high speeds. This means adult tuna can easily cover the scale of Omani shelf just in a few days. In this regard, we were interested in data featuring the thermal structure of tuna habitat. Data on the vertical distribution of temperature in the upper 300m layer were retrieved from the historical database we assembled, for the western Arabian Sea, including the Omani shelf region (Table 2 and Figure 1).

**Table 2.** Research vessels and cruises assembled and contributed to the historical database on CTD casts. \*NAVY research vessels: MT MITCHELL, AYLWIN. BAINBRIDGE, BROWN, BROWNSON, BRUMBY, CAPODANNO, DECATUR, ESSEX, FANNING, HEWES, J., KITTY HAWK, LA SALLE. MOBILE BAY, MULLINNIX, NEW, NOA, PASSUMPSIC, EARY, R. E., PHARRIS, REQUISITE, SEMMES, STRIBLING, TANNER, USS GEORGE K. MACKENZIE, VALDEZ, VOGELGESANG, ARCO JUNEAU, KIRK, KOELSCH, LAWRENCE, MOALE, MONTGOMERY, E., PAUL, TAYLOR, AIRCRAFT, BERKELEY, HOLT, H. E. SOMERS, and BEAUTEMPS-BEAUPRE.

Country	Institution	R/V name and cruise #	Year
UK	BODC	DISCOVERY(D10)	1994
UK	BODC	DISCOVERY(D12)	1994
UK	UKNO	DALYMPLE	1960,1963
UK	UKNO	HYDRA	1976,1984
UK	UKNO	ROYAL NAVY NON-SURVEY VESSELS	1960,1995
UKRAINE	МНІ	MIKHAIL LOMONOSOV, 19	1966
UKRAINE	IBSS	PROFESSOR VODYANITSKIY, 30	1990
UKRAINE	YugNIRO	NAUKA	1967-1980
UKRAINE	YugNIRO	SKIF	1969-1970
USA	NODC	THOMAS G. THOMPSON (TTN-043)	1995
USA	NODC	THOMAS G. THOMPSON (TTN-045)	1995
USA	NODC	THOMAS G. THOMPSON (TTN-049)	1995
USA	NODC	THOMAS G. THOMPSON (TTN-050)	1995
USA	NODC	THOMAS G. THOMPSON (TTN-053)	1995
USA	NODC	THOMAS G. THOMPSON (TTN-054)	1995
USA	NODC	USCGC RELIANCE	1961
USA	NODC	COMMANDANT ROBERT GIRAUD	1961
USA	NODC	KNORR	1995
USA	WHOI	ESSO AFRICA	1976
USA	WHOI	ESSO GENEVA	1976-1977
USA	WHOI	ESSO KAWASAKI	1975-1977
USA	WHOI	ESSO WILHELMSHAVEN	1976-1977
USA	WHOI	ESSO HONOLULU	1976,1979

Country	Institution	R/V name and cruise #	Year
USA	WHOI	ESSO MADRID	1978-1977
USA	US NAVY SHIPS OF OPPORTUNITY	NAVY SHIPS*	1960,1992
GERMANY	FM-GEOMAR	METEOR 32_1	1995
GERMANY	FM-GEOMAR	SONNE 89_1	1993
GERMANY	FM-GEOMAR	METEOR 32_4	1995
GERMANY	FM-GEOMAR	METEOR 32_6	1996
GERMANY	FM-GEOMAR	METEOR 74_3	2007
GERMANY	FM-GEOMAR	SONNE 118	1997
GERMANY	FM-GEOMAR	SONNE 119	1997
GERMANY	FM-GEOMAR	SONNE 120	1997
THE NETHERLANDS	NIOZ	TYRO, LEG D2	1992
THE NETHERLANDS	NIOZ	TYRO, LEG D3	1992
PAKISTAN	NIOPK	NASEER1	1992
PAKISTAN	NIOPK	NASEER2	1992
PAKISTAN	NIOPK	NASEER3	1993
PAKISTAN	NIOPK	NASEER4	1994
PAKISTAN	NIOPK	NASEER5	1994
JAPAN	JODC	UMITAKA MARU	1994
CANADA	CANADIAN NAVY	ROYAL CANADIAN NAVY SHIPS	2001-2005
FRANCE	NHOS	BEAUTEMPS-BEAUPRE	2004-2010
AUSTRALIA	AUSTRALIAN NAVY	ROYAL AUSTRALIAN NAVY SHIPS	2001-2010
OMAN	MSFC	COASTAL WATERS STATIONS	2001-2010
USA	FREE-DRIFTING PROFILING FLOATS	ARGO	2002-2018
UK	HYDRO DEPARTMENT (BRITISH HYDROGRAPHIC OFFICE)	ROYAL NAVY NON-SURVEY VESSELS	2011-2018

Country	Institution	R/V name and cruise #	Year
FRANCE	NHOS	BEAUTEMPS-BEAUPRE	2011-2014
AUSTRALIA	AUSTRALIAN NAVY	ROYAL AUSTRALIAN NAVY SHIPS	2011-2014
AUSTRALIA	AUSTRALIAN BUREAU OF METEOROLOGY (ABOM)		2012-2013

Over 70% of the data collected in the aforementioned database originate from US and UK expeditions. In order to evaluate decadal changes, these data were arranged in the form of decadal subsets, from 1950s to the present.

Historical records on landings of large and small pelagic fishes and on the number of boats involved in artisanal fishery, come from the archives of the Ministry of Agriculture and Fisheries. Landings have been recorded by categories entitled in archived materials as "Large pelagics", "Small pelagics", "Demersal", "Unidentified Fishes", and etc. Within these categories, fish is distributed over taxonomic groups, such as: "Yellowfin Tuna", "King Fish", "Queenfish", "Sardines", and etc. Data were published in the form of annual reports (Fisheries Statistic Book, 2013).

The "Statistica" v.9 software was used for the Principal Component Analysis, Multiple Stepwise Ridge Regression analysis and the Spectral Analysis. The PASTv.3.25 software (https://www.softpedia.com/) was used to run the Mann-Kendall test and the Lomb periodogram; both applied, to assess characteristics of interannual fluctuations of tuna catches.

### **RESULTS**

We analyzed statistical linkages between monthly and annual time series of tuna catches and environmental variables which we presumed to be potentially important, in mediating tuna catch variations over seasons and years. The environmental variables we selected, set up a system of hierarchically organized ocean-atmosphere interactions, with a special reference to fishery. For example, the wind field impacts sea level pressure, sea surface temperature and surface current velocities. In turn, the wind-driven currents generate mesoscale eddies coupled with the main geostrophic flow, in particular, the Oman Coastal Current; the main one propagating along the Omani shelf overlooking the Arabian Sea (Shi et al., 2000). A geostrophic flow, coupled with the field of eddies, affects the spatial distribution of phytoplankton, which is the main component of sardine diet. In turn, a sardine population is a food source for Yellowfin tuna.

# Physicochemical characteristics of tuna habitats

The Oman Coastal Current (the East Arabian Current) exhibits a relatively narrow range of temperature and salinity variations in the T-S diagrams characterizing currents and water masses of the Arabian Sea. The temperature and salinity varied from 15 to 27°C and from 35.2- 36.1, with a maximal magnitude in the upper layers, along the isopycnal surface of 23kg m<sup>-3</sup>. The flow is well pronounced during the Southwest Monsoon, and is shown, schematically, on Figure 1.

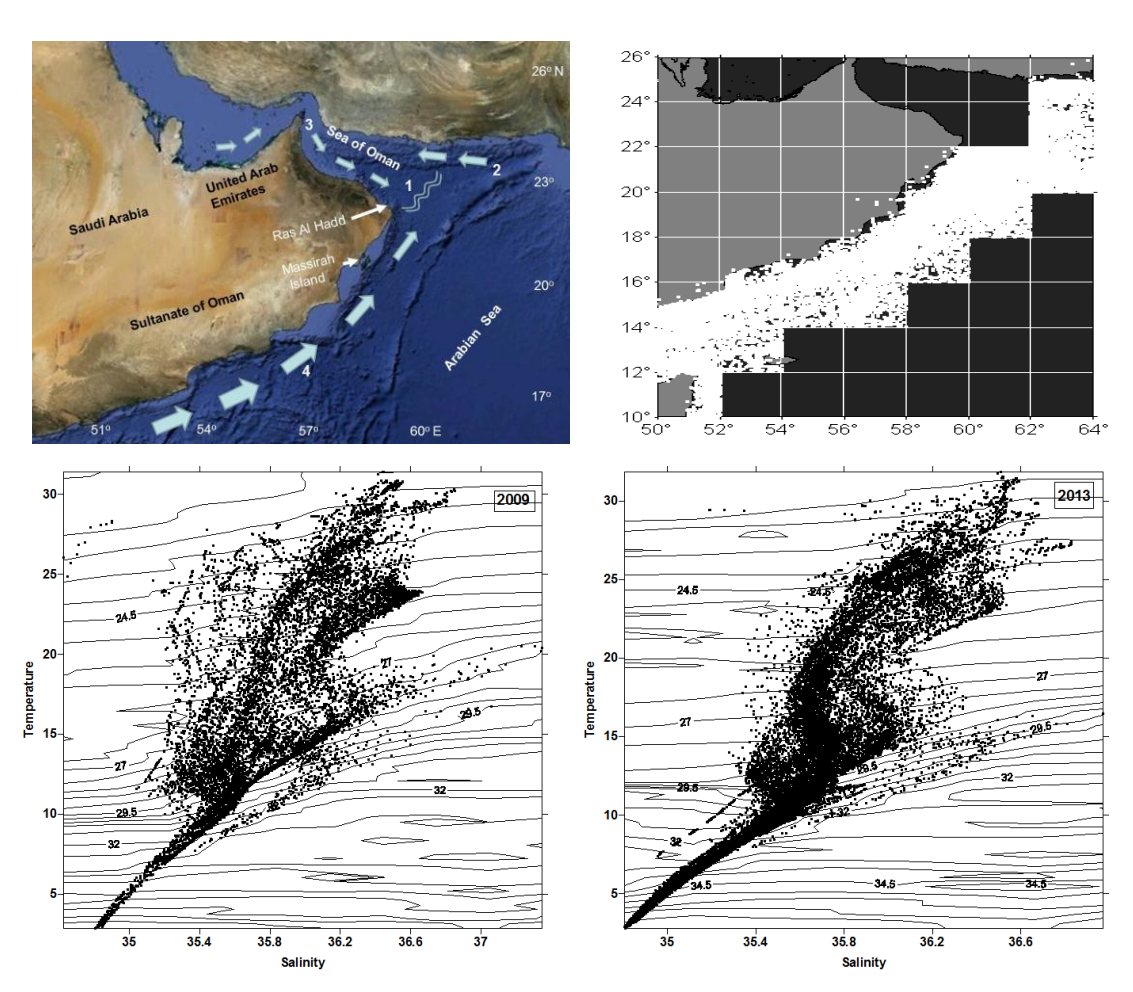


**Figure 1.** <u>Left upper panel</u>: Background image stands for a three-dimensional bathymetric map (www.earth.google.com). Two parallel zigzags (1) demarcate the location of the Ras Al Hadd frontal zone formed by the confluence of the East Oman Current (3) and Oman Coastal Current (4). Arrows (2-4) indicate direction of currents during the Southwest Monsoon. (2): inflow of the Indian Ocean Water mass, (3): outflow of the Persian Gulf Water mass. <u>Right upper panel</u>: location of oceanographic stations (n) with vertical profiles of temperature (from 1950 to 2019) assembled in the database (Table 2). <u>Left and right low panel</u>: T-S diagrams of the Southwest Monsoon season (June-August, 2009 and 2013; n=213 and 478, respectively).

Fragments of temperature, salinity and density we retrieved from the database and represented in the form of T-S diagrams, characterize the Southwest Monsoon thermo-haline structure of water masses and currents, including the Oman Coastal Current. The later one represents an extension of the Somali Current coming from the south. The Oman Coastal Current is the main habitat of the tuna populations subjected to Omani artisanal fishery. The geostrophic velocity of this current exhibits maximal values over the southern part of the Omani shelf and fades northward, as reflected (schematically) by arrow width, on Figure 1.

## Seasonal variability

Monthly catches of Yellowfin Tuna along the Omani shelf overlooking the Arabian Sea have a seasonal trend, in which the spring inter-monsoon maximum is well pronounced (Figure 2). A minor peak was associated with the fall inter-monsoon season. The 5-fold difference in catches characterizes the seasonal cycle. On average, the main peak contributed from 9 to 32%, of the annual catches in 2002-2018.

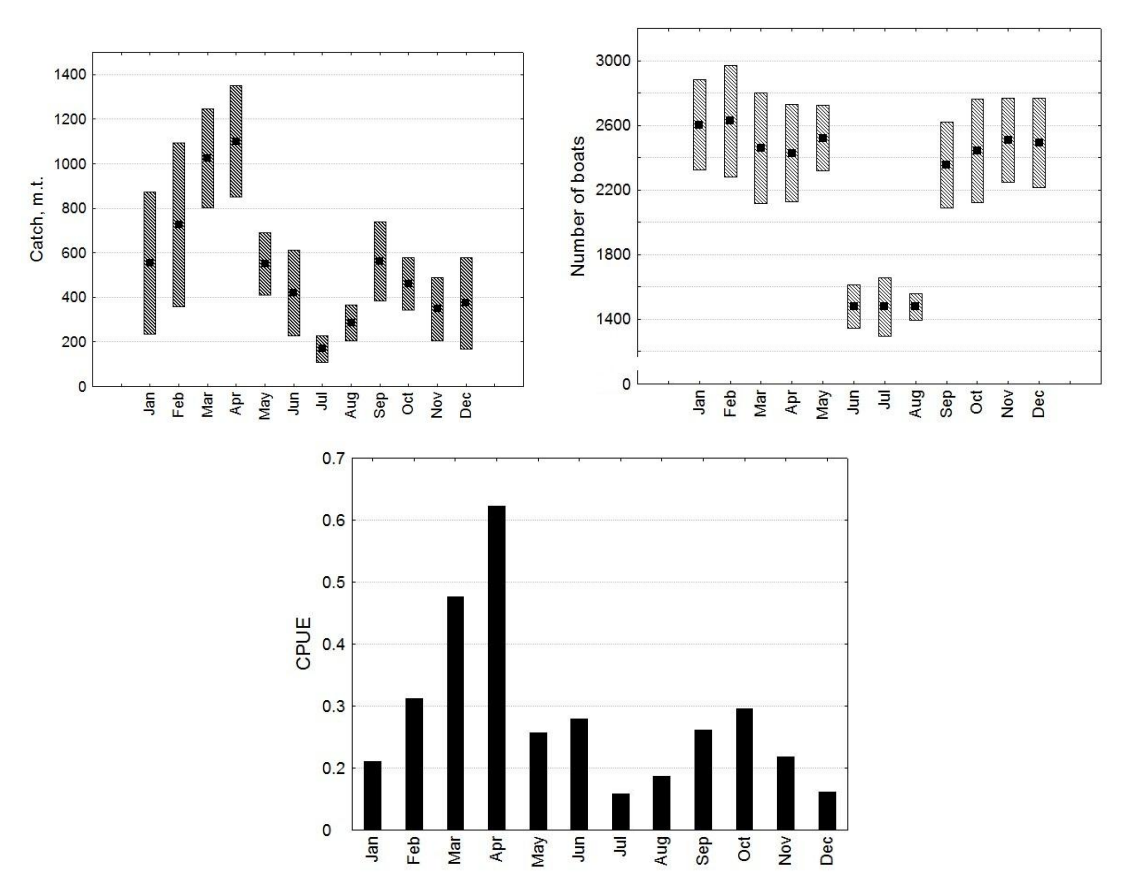


**Figure 2.** Seasonal variations of Yellowfin tuna catches in the Arabian Sea (upper left panel), the number of boats involved in fishery (upper right panel) and catch per unit of effort (mt/boat; low panel). Black squares of the upper panel figures stand for monthly means. Shaded areas stand for means  $\pm$  two standard errors.

The seasonal pattern of fishing effort showed a marked decline during the time of rough weather at sea associated with the Southwest Monsoon. The number of boats stayed invariant during all other months, with no statistical difference between them. This means that the seasonal trend of fishing effort could not fully explain the increase of catches observed from January through April.

For the assessment of statistical coupling between multiple environmental variables, which potentially contributed to a seasonal trend, the Varimax normalized matrix of the Principal Component Analysis was computed. The Varimax procedure amounts to a variance maximizing rotation of the original variable space. The transformed products were further treated as the measures of similarity between variables implying similar seasonal pattern. The extraction of eigenvectors enables one to reduce the diversity of numerous variables to a few Principal Components (Factors) in which the component scores are standardized units based on a correlation matrix. In other words, the eigenvectors are the results of the projection of the original variable axes into the space of new Principal Components.

We constrained the analysis by the extraction of two factors (principal components F1 and F2), which explained 71% of the total variance in the system of selected variables exhibiting seasonal changes (Table 3).

**Table 3.** Factor loading and statistical coupling in seasonal variations of selected parameters. Eigenvalues: 7.03 and 4.42.

Variables	F1	F2
Tuna (catch per unit of effort)	-0.31	0.81
Sardines (catch per unit of effort)	0.75	-0.22
Concentration of dissolved oxygen	-0.71	-0.08
Atmospheric pressure at sea surface	0.36	-0.08
Sea surface temperature gradient (west-east)	0.87	0.42
Zonal component of the wind speed	0.91	0.20
Meridional component of the wind speed	0.95	0.15
Concentration of chlorophyll-a	0.60	-0.42
Meridional component of the current velocity	0.94	0.28
Zonal component of the current velocity	0.86	-0.10
Cyclonic eddies	-0.25	0.75
Anticyclonic eddies	0.38	0.72
Photosynthetically available radiation	0.45	0.84
Mixed layer depth	0.45	0.84
Concentration of dissolved nitrates	0.67	-0.34
Outgoing longwave radiation	-0.24	0.88

Statistically significant loading exceeding 0.7 were marked in bold, in the Table 3. With this regard, one can notice that F1 is contributed mainly by seasonal variations of the meridional and zonal components of the wind speed, geostrophic current velocity, sea surface temperature, dissolved oxygen concentration and sardine catches. Tuna catches were associated with the second group of variables (Factor 2) and exhibited statistical coupling with the seasonal variation of the amount of cyclonic eddies, anticyclonic eddies, mixed layer depth, photosynthetically available radiation and outgoing longwave radiation. The "tuna-related factor" (F2), in which tuna has accounted for a maximal statistical load, has contributed 30% into the total variability of the proposed system of variables.

Cyclonic and anti-cyclonic eddies affect the vertical distribution of the dissolved oxygen concentration, which is an important factor for tuna metabolism. In providing further insights into the coupling of these variables, we retrieved vertical profiles of the dissolved oxygen concentration from cruise reports of five consecutive seasonal field surveys carried out along the Omani shelf. The depth of the 2ml L<sup>-1</sup> oxygen concentration featuring a physiological threshold for tuna was estimated, over seasons (Figure 3).

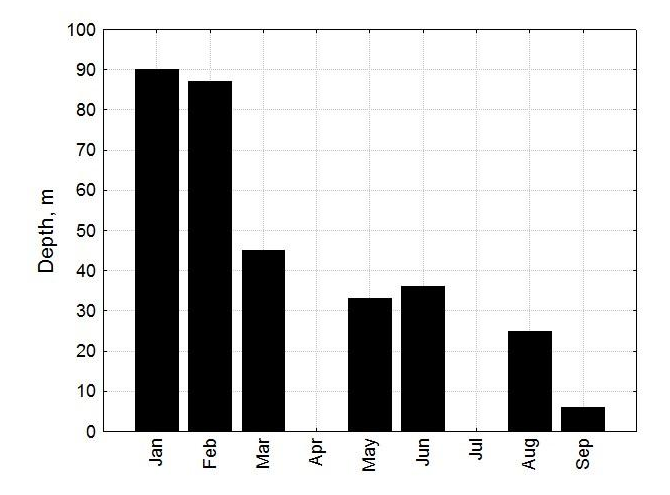
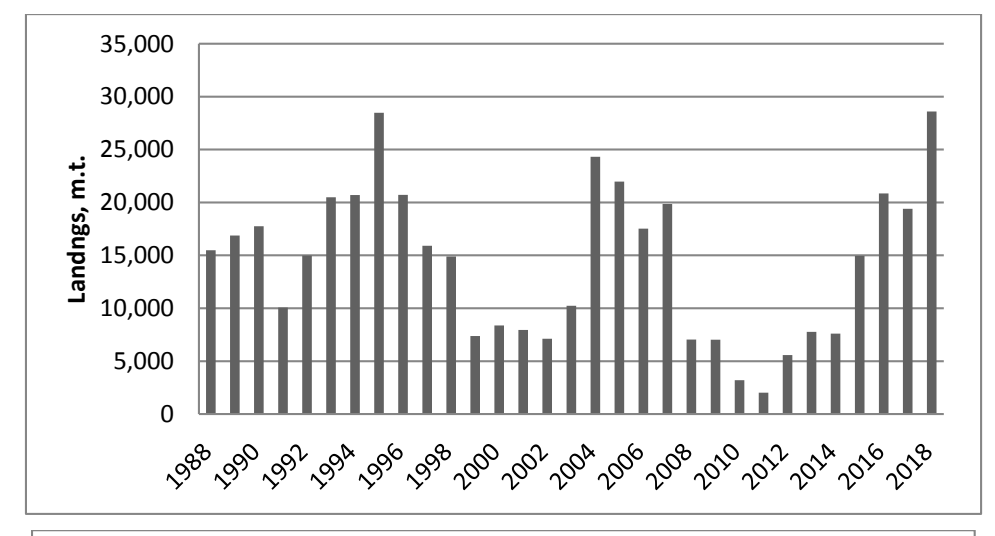


**Figure 3.** Seasonal variation of the depth of 2ml L<sup>-1</sup> concentration of the dissolved oxygen in the Omani shelf waters.

Vertical profiles (not shown here) lined up over seasons, have implied the seasonal shoaling of the dissolved oxygen isopleths. In particular, the concentration of 2 ml L<sup>-1</sup> shifts up, from the depth of ~90 m in January to ~5 m in September. This phenomenon points to a periodic (seasonal) compression of the large pelagic fish habitat. Seasonal maps (shown in Piontkovski and Al Oufi, 2014) implied a marked patchiness pronounced in the distribution of dissolved oxygen concentration over the Omani shelf area. Seasonal patchiness of oxygen distribution should affect the aggregation of tuna over the shelf area.

# Interannual variability

Internannual variations of tuna catches consist of two major components: the long-term trend and deviations from the trend (Figure 4). We believe the trend of the past three decades (which is the 2-fold increase of landings) is associated mostly with the fishing effort (characterized by the 4-fold linear increase of the number of boats involved), while interannual deviations from the trend could be attributed to environmental factors. The Mann-Kendal test (with S=64, Z=1.02, and p=0.31) showed no trend pronounced, in the CPUE annual time series (the catch per unit of effort). These time series have demonstrated irregular fluctuations, with peaks pronounced in 1995, 2004 and 2018, (although the later one still not resembled entirely). Although the 30 year time series of tuna catches is still relatively short for a statistical assessment of the main period pronounced, a pilot analysis (in the form of the Lomb periodogram) implied a periodicity of about 10 years, as a characteristic one.



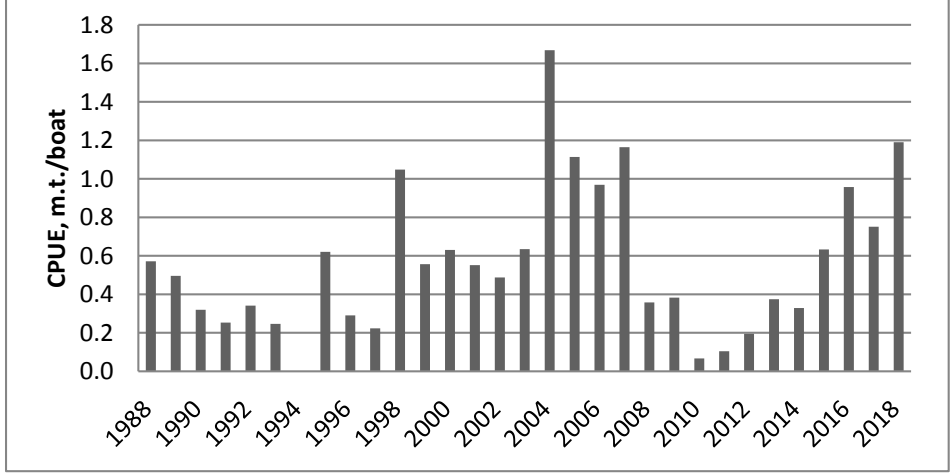


**Figure 4.** Interannual variations of Yellowfin tuna landings (upper panel) and catch per unit of efforts (lower panel) in the Arabian Sea.

Similar (by timing) peaks were also observed in landings of the other large pelagic species (namely "Barracuda", "King Fish" and "Queenfish", in the historical records available from the Fisheries Statistic Book, 2013-2018, but not shown here). In analyzing annual time series of the aforementioned environmental variables, we run the Principal Component Analysis and the Multiple Regression Analysis, in the form of Forward Stepwise Ridge Regression. The Principal Component Analysis elucidated three groups of variables (Factor 1, Factor 2 and Factor 3), which explained 70% of the total variability in tuna catches (Table. 4).

**Table 4.** Factor loading and statistical coupling in interannual variations of selected parameters. Eigenvalues: 5.21, 4.11 and 4.05. Statistically significant loading exceeding 0.7 are marked in bold.

Variables	<b>F</b> 1	F2	F3
Tuna (catch per unit of effort)	0.73	-0.17	0.38
Sardines (catch per unit of effort)	-0.82	-0.24	0.31
Atmospheric pressure gradient at sea surface	0.16	-0.14	0.83
Sea surface temperature (eastern part of the region)	0.03	0.46	0.86
Sea surface temperature gradient (west-east)	-0.06	0.78	0.52
Sea surface temperature (western part of the region)	0.12	-0.30	0.74
Zonal component of the wind speed during Southwest Monsoon	0.73	-0.44	0.08
Meridional component of the wind speed during Southwest Monsoon	0.82	-0.01	0.00
Chlorophyll-a concentration	0.26	-0.65	0.06
Meridional component of the current velocity	0.20	-0.61	0.63
Zonal component of the current velocity	-0.25	-0.83	0.08
Cyclonic eddies	-0.81	0.06	0.25
Anticyclonic eddies	-0.66	0.22	0.26
Photosynthetically available radiation	-0.30	0.05	0.08
Mixed layer depth	-0.54	-0.63	0.18
Concentration of dissolved nitrates	0.78	0.16	0.41
Outgoing longwave radiation	0.69	0.22	0.05
El Niño-Southern Oscillation index	-0.07	0.02	0.90
Indian Ocean Dipole index	-0.10	0.94	0.15

As the variable, Tuna has contributed to the first group (Factor 1: 27%), in which statistical linkages of tuna with sardines, wind speed, cyclonic eddies and concentration of nitrates formed the major factor load. Factors 2 and 3 contributed equally (22 and 21%), to the total variability. The Indian Ocean Dipole and the El Niño-Southern Oscillation index were the two most powerful contributors to these two factors. It should be noted that the time series of both indices were retrieved of the period of spring inter-monsoon which is the time of maximal tuna catches (Figure. 2).

All statistically significant components of Factor 1, 2 and 3 are highly variable. For instance, the wind blowing over the Omani fishery regions is extremely strong during the Southwest Monsoon and fades during the spring inter-monsoon period, which results in a characteristic oscillation pattern (Figure 5). The spectral analysis of time series identified the annual period as the dominant one, followed by the semiannual period, which reflected the contribution of the Northeast Monsoon. The magnitude of interannual variations is less pronounced, visually. However the fragment of time shown is relatively short. The wind direction also exhibits seasonal and interannual variability. The switch of the monsoonal winds (from the southwest to the northeast direction) is well pronounced (Figure 5). Both parameters play a marked role in modulating characteristics of the geostrophic flow along the Omani shelf (the Oman coastal Current) and associated eddies.

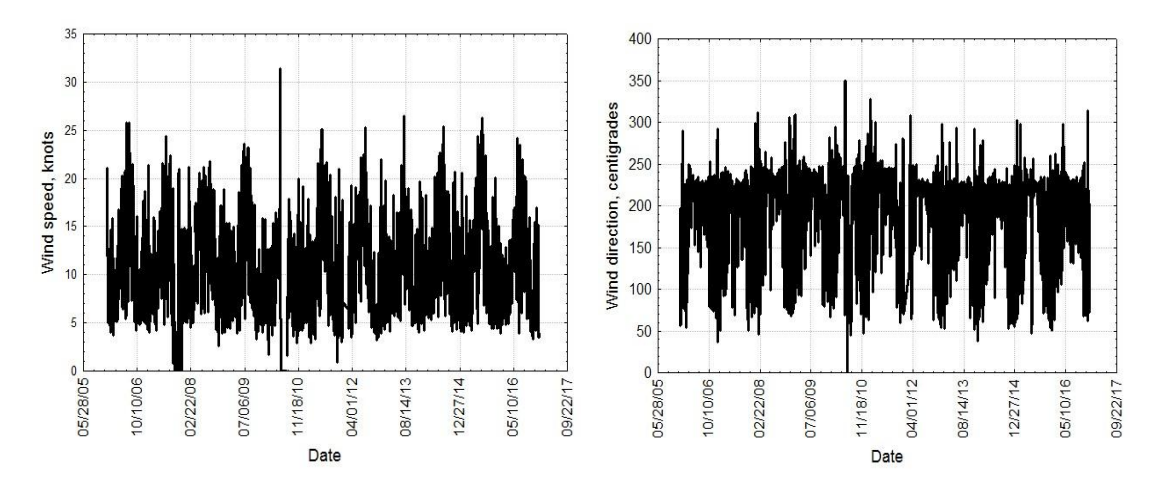


**Figure 5.** A fragment of daily time series of the wind speed and wind direction for the western Arabian Sea region (Masirah Island). Data courtesy from the Ministry of Environment and Climate Affairs (Oman).

As far as the occurrence of mesoscale eddies is concerned, the seasonality of eddy occurrence fits that of tuna catches. In particular, a bimodal pattern, with the peaks observed during fall and spring inter-monsoon seasons was observed (Figure 6). The correlation between the seasonality of tuna catches and the amount of cyclonic eddies in the region was fairly high (r= 0.7, p=0.02), whereas the coefficient of correlation

was lower in the case of anticyclonic eddies (r=0.4, p=0.02). Blue and red colors on the map of sea surface height anomalies contour the location of cold (cyclonic) and warm (anticyclonic) eddies, respectively.

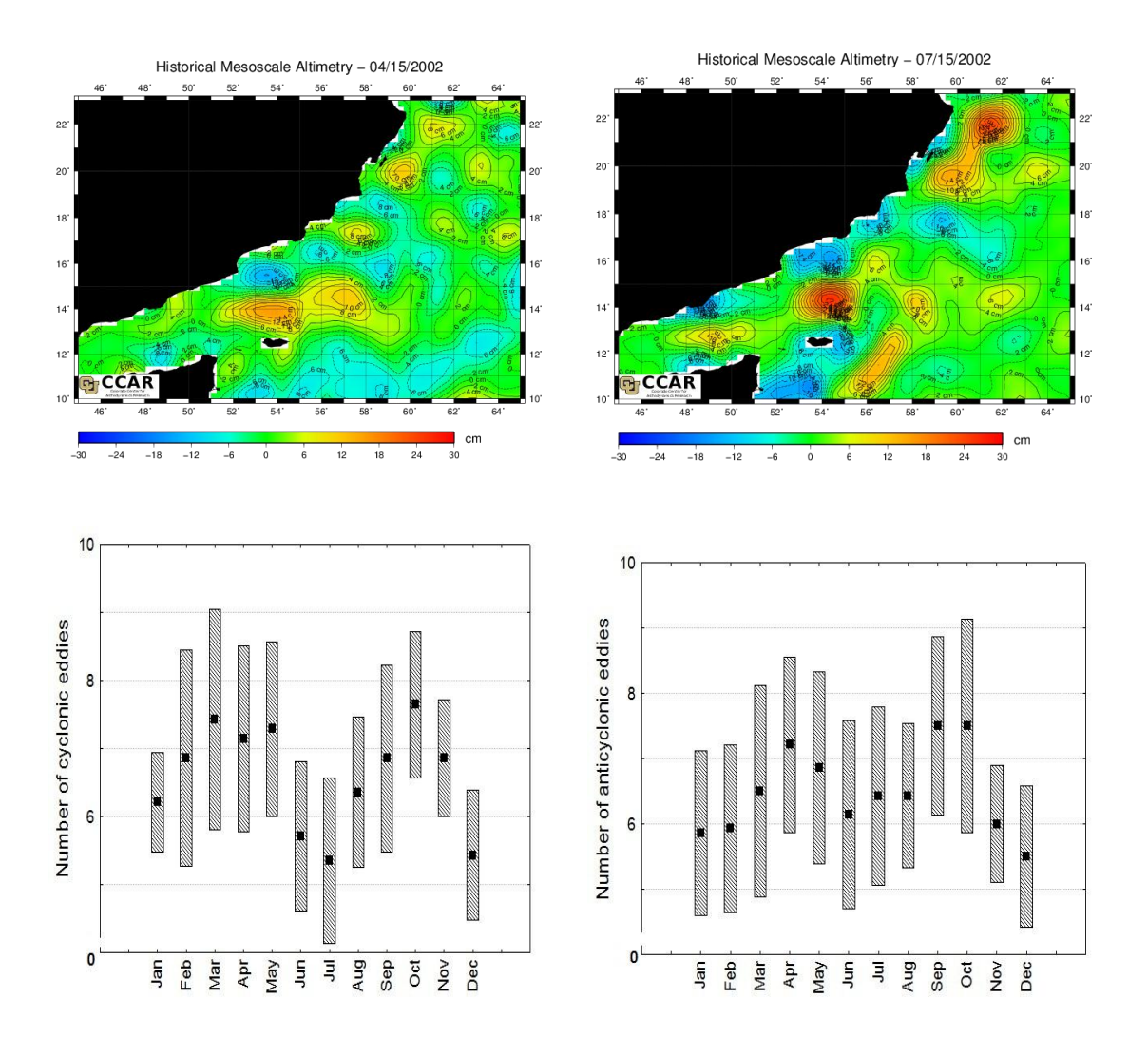


**Figure 6.** Spatiotemporal characteristics of the eddy field. <u>Upper panel</u>: fragments of eddy field exemplified by sea surface height anomalies for the 15<sup>th</sup> of April, 2002 and the 15<sup>th</sup> of June, 2002. Color scale stands for sea surface height anomalies (cm) and illustrates cold (blue color) and warm (orange and red color) eddies contoured by izolines of sea surface height anomalies. Maps were acquired from the CCAR Global Near Real-Time SSH Anomaly/Ocean Color Data Viewer. <u>Low panel</u>: seasonal changes of cyclonic and anticyclonic eddy occurrence in the western Arabian Sea (Piontkovski and Al-Hashmi, 2018). Black squares of the low panel figure stand for monthly means. Shaded areas stand for means ± two standard errors.

On an interannual scale, remotely sensed time series of sea surface height anomalies are still relatively short. Nonetheless, the 13 year data set implied the tendency of eddy occurrence to increase over years, during spring and fall inter-monsoon periods (Piontkovski et al., 2019). In combining seasonal and inter-annual variability, a statistical link between the amount of cyclonic eddies and tuna catches could have an oscillating pattern; it appears during inter-monsoon seasons and fades during monsoons.

The variables contributing the main load to Factor 1, 2 and 3 (Table 4) were subjected to the Multiple Ridge Regression Analysis. The later one implied a statistical significance of the amount of cyclonic eddies, which explained 68% of interannual fluctuations of Yellowfin tuna catches (at lambda= 0.1; R<sup>2</sup>=0.68, p=0.02). Numerous remotely sensed images of sea surface height anomalies (exemplified fragmentary, by Figure 6) show that a couple of eddies, with a characteristic diameter of ~100-200 km, passing along or across a narrow Omani shelf, could cover about half of its area and could modulate frontal zones of various direction. Therefore the potential impact of mesoscale eddies on tuna aggregations should be huge. Eddies observed in the western Arabian Sea (and over the Omani shelf) have a multilateral origin. Some of them are induced by a regional circulation. For instance, a steady spatial pattern consisting of two eddies (cyclonic to the north and anticyclonic to the south of the Ras al Hadd frontal jet), caused by the confluence of regional currents, was observed seasonally, near the Ras al Hadd cape of the Omani coast (Böhm et al.,1999; L'Hegaret et al., 2013). The southern part of the coast has well pronounced capes (namely Ras Madrakah, Ras Sharbatat and Ras Mirbat) which favor the generation of eddies by the main geostrophic flow (the Oman Coastal Current) passing by and fleshing capes.

Along with that, truly oceanic mesoscale eddies mediated by westward propagating Rossby waves were reported. These types of eddies are induced by baroclinic instability of currents in the Arabian Sea, which generates a densely packed eddy field on the western side of the Arabian Sea (Subrahmanyam and Robinson, 2000). The other two parameters that nearly reached a statistically significant level of contribution to the interannual variability of tuna catches were the zonal wind speed and the sea surface temperature.

A fragment of the observed versus predicted by the Ridge Multiple Regression values, in the time range from 2000 to 2015, implies these fluctuations of tuna catches to be well correlated (Figure 7). Values in 2009-2010 exhibited relatively short time range with decoupled fluctuations.

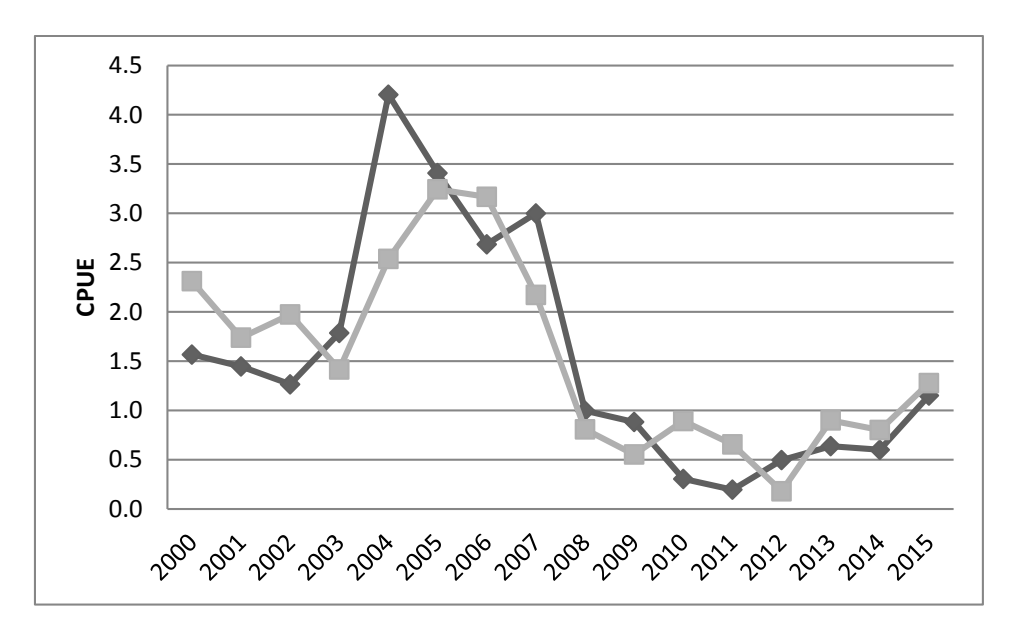


**Figure 7.** A fragment of the observed versus predicted (by the regression model) catches. Multiple R = 0.80,  $R^2 = 0.64$ , p < 0.05.

Whilst cyclonic eddies explained the major part of interannual variations of normalized tuna catches (catch per unit of effort), the unexplained part deals, presumably, with global scale and basin scale atmospheric anomalies, contributing indirectly (through the impact on thermo-haline structure and regional circulation). The El Niño-Southern Oscillation (ENSO) is an anomaly that involves fluctuations in the equatorial Pacific, between warmer than normal sea surface temperatures in the eastern equatorial Pacific (corresponding to the El-Niño phase) and cooler than normal temperatures in the central equatorial Pacific (which is the La-Niña phase). ENSO is the most powerful phenomenon affecting the globe. The anomaly gets well pronounced in the sea surface temperature of the World Ocean. Since 2000, for instance, 6 El-Niño events have been observed.

The Indian Ocean Dipole (IOD) is characterized by anomalously cold sea surface temperatures in the south-eastern part of the Equatorial Indian Ocean versus the anomalously warmed south-western part. Fluctuations of sea surface temperature mediated by the dipole are driven by changes of the wind field of the central equatorial Indian Ocean. In response to anomalies of the wind field, the thermocline rises in the eastern and deepens in the western parts of the basin. In the Arabian Sea, amplitudes of variations of the mixed layer and thermocline depths achieve tens of meters (Ravichandran et al., 2012).

We retrieved annual time series of El-Niño and IOD index from appropriate databases and proposed a scenario of the relationship, in the form of a three-dimensional diagram representing interannual variations of tuna catches as the function of El-Niño Southern Oscillation, and Indian Ocean Dipole (Figure 8).

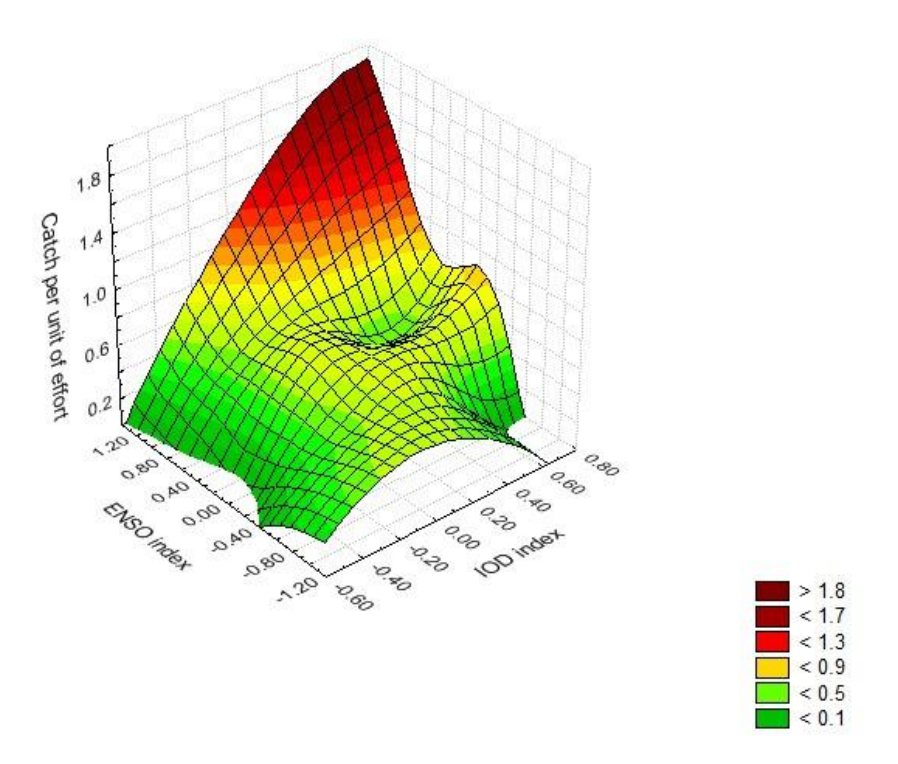


**Figure 8.** Relationship between Yellowfin tuna catch (1988-2018), El-Niño Southern Oscillation, and Indian Ocean Dipole indices. The diagram is smoothed by the Distance Weighted Least Squares method.

Interestingly, the maximal tuna catches of the past 30 years (shown as the red zone) were observed only at a certain combination of ENSO and IOD characteristics. In particular, the ENSO index, ranging from 0.8 to 1.2, and accompanied by the IOD index ranging from 0.6 to 0.8, form the "match" which corresponded to maximal catches. This points out that a certain "numeric match" of two atmospheric anomalies should happen, to favor maximal tuna catches. An intermediate zone of the three-dimensional diagram (with index values from 0.2 to 0.4) characterizes a "numeric mismatch" in the interplay of two atmospheric anomalies, which suppresses tuna catches. The "match-mismatch" events, coupled with the other group of PCA-selected variables, modulate the success of Omani tuna fishery.

## Decadal variability

Presumably, along with interannual fluctuations modulated by global atmospheric anomalies, the Omani tuna catches are subjected to the impact of decadal fluctuations of environmental variables. Relatively short historical records of catches do not allow us to elucidate the decadal trend. However, we might come up with a hypothesis linking the observed interdecadal trends of environmental parameters with expected in tuna catches by the end of 21<sup>st</sup> century. Temperature is one of the key parameters modulating the dynamics of tuna populations. The upper level of optimal temperature

range for adult Yellowfin tuna is ~28°C (Boyce et al., 2008), while the range of temperatures for moderate to high survival in first-feeding larvae is situated between 26°C and 31°C (Wexler et al., 2011). With this regard, we reconstructed an interdecadal trend of tuna habitat temperature for the western Arabian Sea, including the Omani shelf (Figure 9).

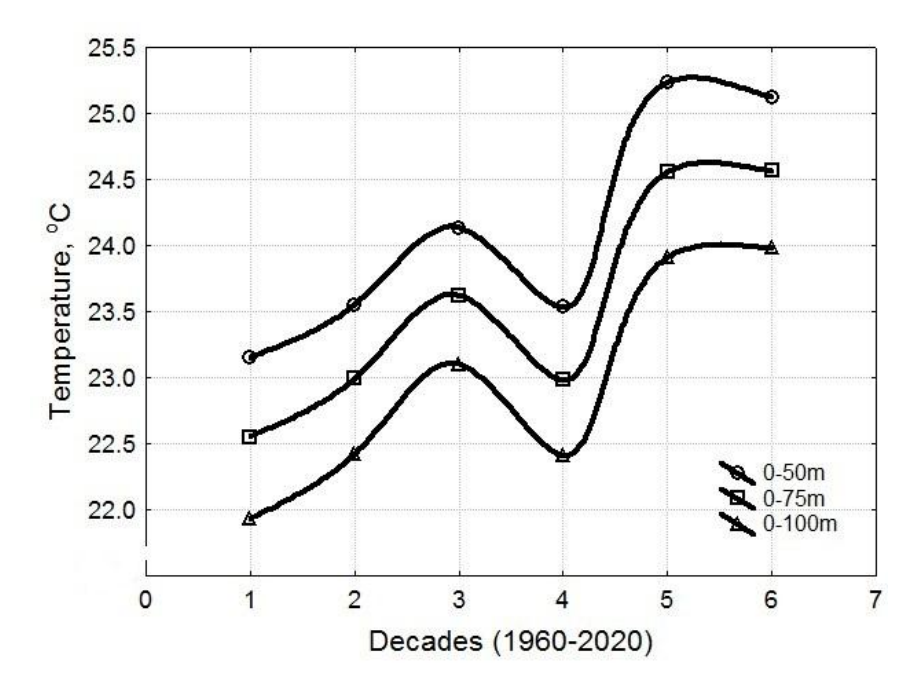


**Figure 9.** Decadal changes of temperature of the Yellowfin tuna habitat in the western Arabian Sea. Number on the X-axis stand for the first through the sixth decade of data (1960-2020). Temperature curves were smoothed by the cubic spline. The number of vertical profiles assembled for the first through the sixth decade = 790, 972, 1277, 1205, 482 and 1156, respectively. The regression equation for 0-100m: Y= $0.04x^4+0.63x^3+6.33x+18.06$  (Chi<sup>2</sup>=0.6, R<sup>2</sup>=0.83, F=1,26, p=0.58).

Historical data presented in Figure 9, span six decades, from 1960s to 2020, with the latest one, yet to be completed. The averaged decadal temperatures are based on 34,242 vertical profiles. A scenario of habitat changes was considered for the width of the upper layer equal to 50m, 75m and 100m. The last versus first decade of data demonstrated the two centigrade increase of the habitat temperature. The trend is statistically significant, according to the Mann-Kendal test, (at S=1 and p=0.03). On one hand, a visual extrapolation of this trend towards the year 2100, would take us to the marginal range of temperatures beyond which the first-feeding larvae as well as adults are physiologically stressed. On the other hand, if the temperature trend displayed on Figure 9 is just a fragment of long-term fluctuation, exhibiting the period of about 12 decades, the temperature of the tuna habitat would cool down, so the end of the 21st century might become thermically favorable for tuna populations.

## **DISCUSSION**

Variations in fish landings incorporate a human-induced and an environmental component both subjected to seasonal, interannual, decadal and other long-term (climate-related) variations. According to the Stock Status Report-2018 of IOTC, the Yellowfin tuna stock in the Indian Ocean is overfished (IOTC, 2018; http://firms.fao.org/firms/resource/22/en). In Oman, the interannual trend of artisanal fishing effort could be estimated, most accurately, for the time range of 1988-2018. The number of boats involved in fishery along the Arabian Sea shelf has exhibited an almost four-fold increase, during this time range. Over 90% of artisanal vessels were fiberglass boats, 5-9 m long (Fishery Statistics Book, 2011, 2013, 2018). Fishing effort varied over shelf regions, however the regional aspect was out of scope of this paper, in which we focused on averaged catches featuring the Arabian Sea shelf.

As for an environmental component, observed events were associated with a regional circulation (contributed by the Oman Coastal Current and mesoscale eddies) and ocean-atmosphere interactions that provided insights into the issue of seasonal and basin scale interannual variability. Numeric simulations resembling the South-west Monsoon implied the Oman Coastal Current width of  $\sim$  150km and velocity of up to 0.7 m s<sup>-1</sup> near the strongest eddies (L'Hegarét et al., 2015).

# Seasonal variability

Seasonal variations of the amount of cyclonic eddies, dissolved oxygen concentration and tuna catches were statistically coupled (contributing markedly to F1 and F2; Table 3). In fact, these links reflect a causative mechanism. Large pelagic fishes, like Yellowfin tuna, are active swimmers sensible to low concentrations of the dissolved oxygen due to their high metabolism. The concentration of less than 3.5 ml L<sup>-1</sup> induces symptoms of stress for many tropical pelagic fishes and is interpreted as the hypoxic threshold (Prince and Goodyear, 2006; Stramma et al., 2012). The concentrations reported for the Yellowfin tuna span the range of 1.5-3.5 ml L<sup>-1</sup> (Brill, 1994; Graham and Dickson, 2004; Sharp, 1978, 1979). Cyclonic eddies of the western Arabian Sea shift the seasonal oxycline upwards and induce spatial heterogeneity in the distribution of the oxygen threshold. Maps of dissolved oxygen concentration based on direct sampling showed "patches" of low oxygen concentration (of about 2 ml L<sup>-1</sup>) associated with eddy location (Piontkovski and Al-Hashmi, 2018; Piontkovski and Al Oufi, 2014). This phenomenon can impact the spatial aggregation of Yellowfin tuna and can explain the relationship between the amount of cyclonic eddies and magnitudes of tuna catches.

The frontal zones formed by the Oman Coastal current as well as fronts on peripheries of mesoscale eddies act as the drivers of tuna aggregation. Yellowfin tuna gather at the warm side of frontal zones (Sund et al., 1981). Remotely sensed sea surface height anomalies in the north-eastern Arabian Sea enabled researchers to predict tuna movements in the water column, both horizontally and vertically. These anomalies (resembling mesoscale eddies) were positively correlated with tuna hooking rates

(Kumar et al., 2015). Tagging of tuna in the southwest Indian Ocean showed that specimens prefer to remain within the mixed layer and to move around the thermocline (Sabarros et al., 2015). In the southern Indian Ocean, the highest 10-year catches of Yellowfin tuna were recorded on the western highly productive edge of a warm-core eddy (Young et al., 2001).

Along with the impact of mesoscale eddies and frontal zones, pelagic fishes inhabiting waters of the western Arabian Sea shelf experience a seasonal lack of oxygen as well as seasonal shoaling of the oxycline (Figure 3). This shoaling induces the compression of the pelagic habitat making fish populations more exposed to fishery.

The mixed layer depth acts as one of statistically significant variables contributing to the Factor 2 of the Principal Component Analysis (Table 3). The deepest mixed-layer depths in the western Arabian Sea were observed during the winter monsoon (Morrison et al., 1998). Also, a 50% decline in the median oxygen saturation near the core of the North Arabian Sea High Salinity Water, from March to August, and even larger between May and November, was noticed for the open waters of the northern Arabian Sea. This seasonal decline was suggested to be renewed early in the year, due to winter convection (Banse and Postel, 2009).

# Interannual variability

The tuna habitat compression by the Oman shelf hypoxia has a seasonal component, nested in an inter-decadal trend of oxycline shoaling. Data from over 50 expeditions incorporating over 2,000 vertical profiles of dissolved oxygen concentration implied the oxycline shoaling, from 153m in the 1960s to 80m in the 2000s (Piontkovski and Al-Oufi, 2015).

A number of reports have implied peaks of tuna landings, in the mid 1990s and early 2000s, in the Somalia region, Mozambique Channel, South Indian Ocean and East Indian Ocean (IOTC, 2017; Herera et al., 2012). These observations match a general pattern of the interannual variations along the Omani shelf (Figure 4). For instance, Nishida et al. (2005) noticed that the peak of catches in 2004 in the Arabian Sea was associated with the shoaling thermocline, which forced tuna to concentrate in the upper layer, thus increasing the catch. The other reason for the high catch might have been a high recruitment observed in 2002 (Lan et al., 2012).

On a basin scale, interplay of atmospheric anomalies (in the form of the El-Niño Southern Oscillation and Indian Ocean Dipole) contribute to tuna aggregations, indirectly. In response to anomalies of the wind field, the thermocline rises in the eastern and deepens in the western parts of the ocean. This mediates the development and fading of warm and cold temperature pools. Warm pools are regions of the highest tuna catches even if primary productivity of the region is low (Lehodey et al., 1997). A statistical population dynamics modeling showed that, in the tropical Pacific Ocean, ENSO-related variability affects the recruitment and total abundance of Yellowfin tuna, which is a result of four mechanisms: the extension of the warm

water pool farther east, enhanced food for tuna larvae due to higher primary production, lower predation of tuna larvae, and retention of the larvae in these favorable areas due to ocean currents. When all the favorable conditions come together, high catches are observed (Lehodey et al., 2006).

The El-Niño Southern Oscillation and Indian Ocean Dipole contribute about 30% and 12% respectively, to the long-term variations of the sea surface temperature in the tropical Indian Ocean (Saji et al., 1999). Interactions between these anomalies are yet to be understood in detail. The ENSO-induced anomalous circulation over the Arabian Sea could be either countered or supported by the Indian Ocean Dipole, depending on the state of the phase and the amplitude of the two (Charabi and Abdul-Wahab, 2009). Interplay of two key phenomena should affect tuna catches, however, the impact of these anomalies has been assessed separately, so far. In the tropical Pacific Ocean, for instance, spatial shifts in the skipjack population were linked to large zonal displacements of the warm pool that occur during ENSO events (Lehodey et al., 1997). The diagram we proposed (Figure 8), implied a provisional scenario of the interplay between the El-Niño Southern Oscillation, Indian Ocean Dipole and tuna landings along the Omani shelf. In constructing the diagram, we assumed that the response of tuna populations to thermal gradients stayed invariant, over three decades.

IOD and ENSO do also impact characteristics of mesoscale eddies, indirectly. In the southeast Indian Ocean, the interannual variation of eddy occurrence was associated with their kinetic energy, which was mediated by fluctuations of regional currents. In turn, the intensity of currents is modulated by the Indian Ocean Dipole, the Southern Annular Mode, and the El-Niňo Southern Oscillation (Jia et al., 2011).

## Decadal variability

In parallel with a statistical approach employed in our paper, researchers use advanced modeling, which couples the basin scale circulation, primary productivity and climate change scenario. In particular, the SEAPODYM model resembles the advection, spawning, migrations, and mortality, which are constrained by environmental data (namely, sea surface temperature, geostrophic currents, primary and dissolved oxygen concentration), spatial distributions micronektonic tuna forage functional groups and three climate scenario models A pilot test of this model applicably to the Yellowfin tuna fishery in the Indian Ocean has resembled the peaks of catches we discussed (Figure. 4), and predicted the tuna stock up to the end of the 21st century (Lehodey and Senina, 2009). With regard to the three different Earth Models under IPCC RCP8.5 climate change scenario, that drives the physical-biogeochemical coupling in SEAPODYM, along with projected decrease in primary productivity, the 50% reduction of the tuna stock is expected, on a basin (Indian Ocean) scale, by the year 2100. The trend is driven by temperature warming, as tuna populations will approach the upper limit of favorable spawning temperature range, in many places with the exception of Omani fishery (Senina et al., 2015). Details of long-term changes of temperature range applicably to the western Arabian Sea (including Omani shelf) were shown in Figure 9, from which we hypothesized and inferred the 120 year period of temperature fluctuations in this region. With this regard, it might be noted that a similar climate-driven period (125 years), along with some others, was reported in a 5000-year record in varved sediments from the oxygen minimum zone off Pakistan, in the northeastern Arabian Sea (Von Rad et al., 1999).

#### **CONCLUSIONS**

Yellowfin tuna catches along the Omani shelf, in 1988-2018, were subjected to a human-induced and environmental forcing subjected to seasonal and interannual variations. Seasonal variations demonstrated a bimodal trend, with a major peak in April and a minor one, in October, observed during spring and fall inter-monsoon seasons. Apart from the seasonality of fishing efforts associated with rough weather during the south-west monsoon, seasonal variations of tuna catches were statistically related to the two groups of environmental factors. The first one incorporated the wind speed, zonal (offshore) gradient of sea surface temperature, geostrophic current velocity, dissolved oxygen concentration and sardine catches (as an indicator of food for tuna). The amount of mesoscale eddies, mixed layer depth, photosynthetically available radiation, and outgoing longwave radiation formed the second group. Both groups explained 71% of observed seasonal variations of the tuna catch.

Due to the four-fold increase in fishing effort, artisanal catches of Yellowfin tuna along the Omani shelf exhibited a two-fold increase over the past three decades. However, the catch per unit of effort did not show a statistically significant increase. Interannual variations of catches exhibited an irregular pattern, with several peaks (in 1995, 2004 and 2018, with the later one still not resembled entirely). Statistical analysis implied 8 environmental variables which modulated these variations. Namely, the wind speed, amount of cyclonic eddies, sardines (an indicator of food resource for tuna), concentration of nitrates, atmospheric pressure gradient, sea surface temperature, El Niño-Southern Oscillation, and Indian Ocean Dipole anomalies. Coupling of these variables explained 70% of interannual variations of Yellowfin tuna catch along the Omani shelf overlooking the western Arabian Sea. The relationship between catches, El-Niño Southern Oscillation and Indian Ocean Dipole index pointed to a certain "numeric match" of two atmospheric anomalies that should happen, to favor maximal tuna catches.

## **ACKNOWLEDGMENTS**

This research was funded by SQU grant # IG/AGR/FISH/17/01. The authors would like to thank colleagues from the Ministry of Agriculture and Fisheries (Oman) for providing data and consultations on fish catches, L.Galkovskaya for assembling CTD profiles, and Dr. Y.Al-Sharabi for comments on the analysis of climate indices.

#### REFERENCES

- [1] Arur, A., Krishmam, P., George, G., Bharathi, M.P.G., Kaliyamoorthy, M., Shaeb, K.H.B., Suryavanshi, A.S., Kumar, T.S., Joshi, A.K., 2014, The influence of mesoscale eddies on commercial fishery in the coastal waters of the Andaman and Nicobar Islands, India. *International Journal of Remote Sensing*, 35, 17, pp. 6418-6443.
- [2] Baird, S.J., Bagley, N., Devine, J., Gauthier, S., McKoy, J., Macaulay, G., and Dunford, A., 2009, Fish Resources of the Arabian Sea Coast of Oman: Habitat, Biodiversity and Oceanography. Technical Report 5. *Bruce Shallard and Associates*. Muscat, 163pp.
- [3] Banse, K., and English, D.C., 2000, Geographical differences in seasonality of CZCS-derived phytoplankton pigment in the Arabian Sea for 1978-1986. *Deep-Sea Research*, II, 47, pp. 1623-1677.
- [4] Banse, K., and Postel, J.R., 2009, Wintertime convection and ventilation of the upper pycnocline in the northernmost Arabian Sea. In: Indian Ocean biogeochemical processes and ecological variability. Wiggert, J.D., et al. (Eds.). *American Geophysical Union*. Washington DC., pp. 87-118.
- [5] Barber, R.T., Marra, J., Bidigare, R., Codispoti, L., Halpern, D., Johnson, Z., Latasa, M., Goerìke R., Smith, S., 2001, Primary productivity and its regulation in the Arabian Sea during 1995. *Deep-Sea Research*, II, 48, pp. 1127-1172.
- [6] Boyce, D.G., Tittensor, D.P., and Worm, B., 2008, Effects of temperature on global patterns of tuna and billfish richness. *Marine Ecology Progress Series*, 355, pp.267-276.
- [7] Böhm, E.; Morrison, J.M.; Manghnani, V.; Kim, H.S. and Flagg, C.N, 1999, The Ras al Hadd Jet: remotely sensed and acoustic Doppler current profiler observations in 1994-1995. *Deep-Sea Research*, II, 46, pp. 1531-1549.
- [8] Brill, R., 1994, A review of temperature and oxygen tolerance studies of tunas pertinent to fisheries oceanography, movement models and stock assessments. *Fisheries Oceanography*, 3, 3, pp. 204-206.
- [9] Charabi, Y, and Abdul-Wahab, S.A., 2009, Synoptic aspects of the summer monsoon of southern Oman and its global teleconnections *Journal of Geophysical Research*, 114, D07107, doi:10.1029/2008JD010234.
- [10] Chelton, D.B., Schlax, M.G., and Samelson, R.M., 2011, Global observations of nonlinear mesoscale eddies. *Progress in Oceanography*, 91, pp. 167-216.
- [11] Fishery Statistics Book, 2011, Sultanate of Oman. *Ministry of Fisheries*. Muscat, 156p.
- [12] Fishery Statistics Book, 2013, General Directorate of Planning & Development. Fisheries Statistics Department. *Ministry of Agriculture and Fisheries*. Muscat, 248p.
- [13] Fishery Statistics Book, 2018, General Directorate of Planning & Development. Fisheries Statistics Department. *Ministry of Agriculture and Fisheries*. Muscat, 240p.

- [14] Graham, J.B., and Dickson, K.A., 2004, Tuna comparative physiology. *The Journal of Experimental Biology*, 207, pp. 4015-4024.
- [15] Herrera, M., Pierre, L., Geehan, J., and Milion, J., 2012, Review of the statistical data and fishery trends for tropical tunas. *Indian Ocean Tuna Comission*, IOTC-2012-WTTT14-07 Rev\_1, pp.1-62.
- [16] Jia, F., Wu, L., Lan, J., and Qiu, B., 2011, Interannual modulation of eddy kinetic energy in the southeast Indian Ocean by Southern Annular Mode. *Journal of Geophysical Research*, 116, C02029, doi:10.1029/2010JC006699.
- [17] IOTC, 2017, Review of the statistical data and fishery trends for tropical tunas. IOTC-2017-WPTT19-07, 47pp.
- [18] Khalfallah, M., Zylich, K., Zeller, D., and Pauly, D., 2016, Reconstruction of domestic marine fisheries catches for Oman (1950-2015). *Frontiers in Marine Science*, 3, 152, doi:10.3389/fmars.2016.00152.
- [19] Kistler, R., Kalnay, E., Collins, W., Saha, S., White, G., Woollen, J., Chelliah, M., Dool, W., Jenne, R., and Fiorino, M., 2001, The NCEP-NCAR 50-Year Reanalysis: Monthly Means CD-ROM and Documentation. *Bulletin of the American Meteorological Society*, 82, pp. 247-268.
- [20] Kumar, P.S., Gopalakrishna, N.P., and Ushadevi, M., 2014, El Nino Southern Oscillation (ENSO) impact on tuna fisheries in Indian Ocean. *Springer Plus*, 3, pp.591-604.
- [21] Kumar, N., Kumar, N., Swetha, N. M., Nayak, J., Bright, R.P., and Kumar, T.S., 2015. Utility of sea surface height anomaly (SSHa) in determination of potential fishing zones. Technical Report ESSO/INCOIS/ASG/TR(02)2015. *INCOIS*, Hyderabad.
- [22] Lan, K-W.,.Lee, M-A., Nishida, T., Lu, H-J., Weng, J-S., and Changi, Y.I., 2012, Environmental effects on yellowfin tuna catch by the Taiwan longline fishery in the Arabian Sea. International *Journal of Remote Sensing*, 33, 23, pp. 7491-7506.
- [23] Lee, P.F., Chen, I.C., and Tseng, W.N., 1999, Distribution patterns of three dominant tuna species in the Indian Ocean. 19<sup>th</sup> International ESRI Users Conference. San Diego, CA.
- [24] Lehodey, P., Bertignac, M., Hampton, J., Lewis, A., and Picaut, J., 1997, El Ninõ Southern Oscillation and tuna in the western Pacific. *Letters to Nature*, 389, pp. 439-468.
- [25] Lehodey, P., Alheit, J., Barange, M., Baumgartner, T., Beaugrand, G., Drinkwater, K., Fromentin, J-M., Hare, S.R., Ottersen, G., Perry, I., Roy, C., van der Lingen, C.D., and Werner, F., 2006, Climate variability, fish and fisheries. *Journal of Climate*, 19, pp. 5009-5030.
- [26] Lehodey, P., and Senina, I., 2009, An update of recent developments and applications of the SEAPODYM model. 5<sup>th</sup> Regular Session of the Scientific Committee of the Western Central Pacific Fisheries Commission. WCPFC-SC5-2009/EB-WP-10.

- [27] L'Hégaret, P., Lacour, L., Carton, X., Roullet, G., Baraille, R., and Corréard, S., 2013, A seasonal dipolar eddy near Ras Al Hamra (Sea of Oman). *Ocean Dynamics*, 63, pp, 633-659
- [28] L'Hegarét, P., Duarte, R., Carton, X., Vic, C., Ciani, D., Baraille, R., Corréard, S., 2015, Mesoscale variability in the Arabian Sea from HYCOM model results and observations: impact on the Persian Gulf Water path. *Ocean Science*, 11, pp. 667-693.
- [29] Mahrooqi, K.K., and Al-Shidhami, M.B.M., 2013, Information on fisheries, research and statistics. Sultanate of Oman National Report to the Scientific Committee of the Indian Ocean Tuna Commission, 2012. IOTC-2013-SC16-NR20.
- [30] Mohri, M., and Nishida, T., 2000, Consideration on distribution of adult yellowfin tuna (Thunnus albacares) in the Indian Ocean based on Japanese tuna longline fiesheries and survey information. *Journal of National Fisheries University*, 49, 1, pp.1-11.
- [31] Morrison, J.M., Codispoti, L.A., Gaurin, S., Jones, B., Manghnani, V., and Zheng, Z., 1998, Seasonal variation of hydrographic and nutrient fields during the US JGOFS Arabian Sea Process Study. *Deep-Sea Research*, II, 45, pp. 2053-2101.
- [32] Nishida, T., Matsuura, H., Shiba, Y., Tanaka, M., Mohri, M., and Chang, S-K., 2005, Did ecological anomalies cause 1993 and 2003-2004 high catches of yellowfin tuna (*Thunnus albacares*) in the western Indian Ocean? *Indian Ocean Tuna Commission*, IOTC-WPTT 2005, pp.1-26.
- [33] Piontkovski, S.A., and Al-Oufi, H.S., 2014, The oxygen minimum zone and fish landings along the Omani shelf. *Journal of Fisheries and Aquatic Science*, 9, 5, pp. 294-310.
- [34] Piontkovski, S.A. and Al-Oufi, H.S., 2015, The Omani shelf hypoxia and the warming Arabian Sea. *International Journal of Environmental Studies*, 72, 2, pp. 256-264.
- [35] Piontkovski, S.A., and Al-Hashmi, K., 2018, Mesoscale eddies and Yellowfin Tuna catches in the Western Arabian Sea. *International Journal of Ecology and Enrironmental Sciences*, 44, 3, pp. 239-250.
- [36] Piontkovski, S.A., Al-Tarshi, M.H., Al-Ismaili, S.M., Al-Jardani, S.S.H., and Al-Alawi, Y.H.A., 2019, Monitoring mesoscale eddies in the western Arabian Sea. *International Journal of Oceans and Oceanography*, 13, pp. 1-23.
- [37] Prince, E.D., and Goodyear, C.P., 2006, Hypoxia-based compression of tropical pelagic fishes. *Fisheries Oceanography*, 15, pp. 451-464.
- [38] Ravichandran, M., Girishkumar, M.S., and Riser, S., 2012, Observed variability of chlorophyll-a using Argo profiling floats in the southeastern Arabian Sea. *Deep-Sea Research*, I, 65, pp.15-25.
- [39] Sabarros, P.S., Romanov, E.V., and Bach, P., 2015, Vertical behavior and habitat preferences of yellowfin and bigeye tuna in the South West Indian

- Ocean inferred from PSAT tagging data. IOTC Report IOTC-2015-WPTT17-42Rev\_1, pp. 1-16.
- [40] Saji, N.H., Goswami, B.N., Vinayachandran, P.N., and Yamagata, T., 1999, A dipole mode in the tropical Indian Ocean. *Nature*, 401, pp. 360-363.
- [41] Senina, I., Lehodey, P., Calmettes, B., Nicol, S., Caillot, S., Hampton, J., and Williams, P., 2015, SEAPODYM application for yellowfin tuna in the Pacific Ocean. Western and Central Pacific Fisheries Commission. Scientific committee Eleven Regular Session, WCPFC-SC11-215/EB-IP-01.
- [42] Sharp, G. D., 1978, Behavioral and physiological properties of tunas and their effects on vulnerability to fishing gear. In: The physiological ecology of tunas, G. P. Sharp and A. E. Dizon (Eds.). New York, Academic Press, pp. 397–450.
- [43] Sharp, G. D., 1979, Areas of potentially successful tunas in the Indian Ocean with emphasis on surface methods. Rome, *FAO*, IOFC/DEV/79/47: 1-55.
- [44] Shi, W., Morrison, J.M., Bohm, E., and Manghnani, V., 2000, The Oman upwelling zone during 1993, 1994 and 1995. *Deep-Sea Research*, II, 47, pp. 1227-1247.
- [45] Stramma, L., Prince, E.D., Schmidtko, .S, Jiangang, L., Hoolihan, J.P., Visbeck, M., Wallace, D.W.R., Brandt, P., and Körtzinger, A. 2012, Expansion of oxygen minimum zones may reduce available habitat for tropical pelagic fishes. *Nature Climate Change*, 2, pp. 33-37
- [46] Stretta, J.M., 1991, Forecasting models for tuna fishery with aeroespatial remote sensing. *International Journal of Remote Sensing*, 12, 4, pp. 771-779.
- [47] Subrahmanyam, B., and Robinson, I., 2000, Sea surface height variability in the Indian Ocean from TOPEX/POSEIDON altimetry and model simulations. *Marine Geodesy*, 23, pp. 167-195.
- [48] Sund, P.N., Blackburn, M., and Williams, F., 1981, Tunas and their environment in the Pacific Ocean: a review. *Oceanology and Marine Biology Annual Review*, 19, pp. 443-512.
- [49] Suzuki, Z., Tomlison, P.K., and Honma, M., 1978, Population structure of Pacific yellowfin tuna. *Inter-American Tropical Tuna Commission Bulletin*, 17, 5, pp. 273-441.
- [50] Von Rad, U., Schaaf, M., Michels, K.H., Schulz, H., Berger, W.H., and Siroco, F., 1999, A 5000-yr record of climate change in varved sediments from the oxygen minimum zone off Pakistan, northeasten Arabian Sea. *Quaternary Research*, 51,1, pp. 39-53.
- [51] Wexler, J., Margulies, D., and Scholey, V., 2011, Temperature and dissolved oxygen requirements for survival of yellowfin tuna, *Tunnus albacares*, larvae. *Journal of Experimental Marine Biology and Ecology*, 404, pp. 6372.
- [52] Young, J.W., Lamb, T.D., Bradford, R.W., and Kloser, R., 2001, Yellowfin tuna (*Thunus albacares*) aggregations along the shelf break off south-eastern Australia: links between inshore and offshore processes. *Marine and Freshwater Research*, 52, 4, pp. 463-474.